

# Cohesion Design-Led Tough Sealants with Controllably Dissolvable Properties

Chaowei Li, Wanglin Duan, Ye Zhu, Guanying Li, Min Gao, Zuquan Weng,\* Yuan Zhu,\* and Yazhong Bu\*



Cite This: <https://doi.org/10.1021/acsami.2c08328>



Read Online

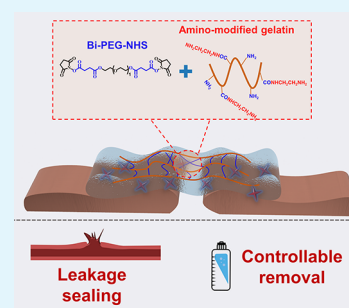
ACCESS |

Metrics & More

Article Recommendations

**ABSTRACT:** Leakage is a common complication of surgeries and injuries, causing pain and increasing the economic burden on patients. Although there are commercially available sealants for leakage prevention, few of them are entirely satisfactory due to disease transmission, high cost, and poor biocompatibility. In addition, none of them can be controllably removed for further healthcare. In this paper, by using cohesion design, a sealant based on amino-modified gelatin (AG) and bi-polyethylene glycol *N*-hydroxysuccinimide active ester (Bi-PEG-SS) was fabricated. To increase the bursting pressure, the cohesion strength was enhanced by increasing the cross-linking density of the sealant. To endow the sealant with controllably dissolvable properties, the smart succinic ester units were introduced into the cohesion network. Both the in vitro and in vivo experiments showed that this sealant processed high bursting pressure with efficient hemorrhage control. Moreover, no side effects were observed after 7 days of in vivo sealing, including little inflammation and fibrogenesis. These results, together with the easy availability of the raw materials, revealed that this sealant might be a promising alternative for leakage sealing.

**KEYWORDS:** sealant, controllable dissolution, succinic ester, bioadhesive, NHS-ester



## INTRODUCTION

Leakage is a common complication of surgeries and injuries.<sup>1,2</sup> For example, post-operative bleeding is a leakage of blood and is of high risk in various surgical procedures.<sup>3</sup> In the field of obstetrics and gynecology, catastrophic bleeding has become the main source of morbidity and mortality for women suffering from placenta accrete spectrum, and sometimes hysterectomy has to be performed to stop the bleeding.<sup>4,5</sup> After lung resections, the incidence of air leakage was reported to be around 50% not only causing suboptimal pain control, nausea, and vomiting but also resulting in a financial cost of approximately €39,000 per patient.<sup>6</sup> Moreover, cerebrospinal fluid leakage and gastric fluid leakage also lead to pain and death.<sup>7</sup> As a result, effectively sealing the leakage is extremely important in the clinic. By 2027, the global market for tissue sealants and hemostats will grow beyond \$10 billion.<sup>3,8</sup> However, the commercialized sealants are still far from satisfactory. Fibrin glue, multiarmed-poly(ethylene glycol) (multiarmed-PEG), and Albumin-based sealants are the primary commercially available sealants. Fibrin-based sealants, made of fibrinogen and thrombin, are the most widely used ones in the clinic. However, they are derived from blood with the potential risk of transferring blood-relevant diseases, and the limited source further increases the cost.<sup>9</sup> There were reports that Fibrin glue caused severe allergic reactions from minutes to days after application.<sup>10,11</sup> Multiarmed-PEG-based bioadhesives include Coseal and Duraseal.<sup>12,13</sup> Although they

showed high bursting pressure with high sealing efficacy, the cost of the multi-armed-PEGs increases the economic burden on the patients.<sup>14,15</sup> Another widely used sealant is the Albumin-based one, which is Bioglue. Bioglue showed extremely high bursting pressure among the commercialized sealants. However, the cross-linking of Bioglue involved 10% of toxic glutaraldehyde and caused complications such as inflammation, nerve toxicity, and tissue necrosis.<sup>16,17</sup> Besides, Bioglue was much stiffer than human soft tissues, restricting normal physiological vascular dilatation and leading to pseudoaneurysms.<sup>18</sup> Easy removal of sealants is also an important property in need of wound re-exposure because traditional mechanical debridement easily leads to second tissue injuries and causes pain to patients.<sup>19,20</sup> However, none of the commercialized sealants express controllably removable properties.

Gelatin is obtained from collagen by controlled hydrolysis, which has similar biological properties as collagen, like supporting cell migration, proliferation, and adhesion.<sup>21</sup> Although with similar functions, collagen use is always concerned with an antigenic response because of its helical structure and the aromatic radicals formed by the high content of tyrosine, tryptophan, and phenylalanine.<sup>22</sup> On the contrary,

Received: May 11, 2022

Accepted: July 11, 2022

gelatin has low antigenicity with low cost and easy availability.<sup>23</sup> Besides, it has good solubility in water, making it a good component for hydrogel fabrication.<sup>24</sup> There are many gelatin-based sealants. However, most of them are cross-linked with toxic cross-linking agents, like glutaraldehyde, formaldehyde, and genipin.<sup>25–28</sup> Moreover, none of them were reported to have controllable dissolution abilities.<sup>29,30</sup>

N-Hydroxysuccinimide-based active ester (NHS-ester) is a cross-linking agent for amino-contained polymers, processing fast reactions with amino groups without particular catalysis and conditions.<sup>31</sup> It was used to fabricate sealants with adhesion to tissues. Generally, multiarmed-PEG-NHS ester was used to cross-link amino-contained polymers for manufacturing sealants because they can form a denser cross-linking network.<sup>32</sup> However, the high price of those cross-linkers further limits their wide applications among patients.<sup>14</sup> Instead of multiarmed-PEG-NHS, we previously used a Bi-PEG-NHS ester to fabricate bioadhesives with gelatin (SEgel) for post-operative anti-adhesion.<sup>33</sup> Compared with traditional multiarmed-PEG-NHS ester, Bi-PEG-NHS ester is more cost effective. However, the relatively low cross-linking density formed by the Bi-PEG-NHS ester prevents SEgel's applications in sealing leakage.

Cohesion design plays a vital role in fabricating sealants. For sealing leakage, a sealant is expected to have high cohesion strength.<sup>34</sup> Besides, by the design of cohesion strategies, functions like removability can be introduced into the sealant systems.<sup>35,36</sup> Hence, in this work, by cohesion design, a new Bi-PEG-NHS ester and gelatin-based sealant were developed with high bursting pressure and controllably removable properties (Scheme 1). To increase the cross-linking density of SEgel, gelatin was modified with more amine groups (AG) and later cross-linked with the Bi-PEG-NHS ester to form SEAgel with higher cohesion strength. To endow SEAgel with controllably removable properties, succinic ester, which is controllably erased by the cysteamine solution (CA), was introduced into the cohesion formation using Bi-PEG-succinimidyl succinate (Bi-PEG-SS) as the NHS ester, inspired by our previous work.<sup>20</sup> It is hypothesized that SEAgel with higher cross-linking density and smart dissolvable units will demonstrate high bursting pressure and controllably dissolvable properties, offering a new alternative to leaking prevention after surgeries.

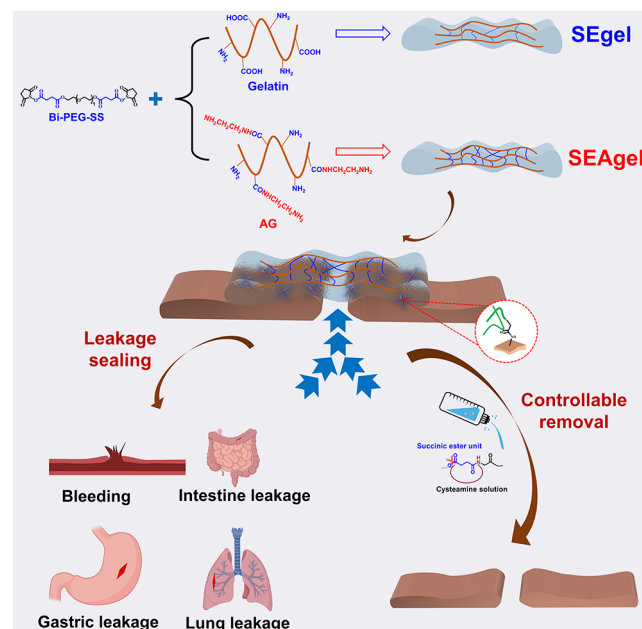
## EXPERIMENTAL SECTION

**Synthesis of AG.** AG was synthesized according to previous reports.<sup>37</sup> To avoid the potential side reactions, gelatin (Type A, Sigma-Aldrich, 10 g) and ethylenediamine (16 mL) were first well mixed in phosphate-buffered saline (PBS) (pH = 5, 100 mL) at room temperature. The pH of the solution was adjusted to 5 when it becomes apparent. Then, EDC (4.6 g) was added to the mixture. The mixture was stirred for 24 h, dialyzed with deionized water for 3 days, and finally, AG was obtained by freeze-drying. The structure of the compound is determined by <sup>1</sup>H NMR measurements.

**Preparation of SEAgel and SEgel Hydrogel.** 25% SEAgel solution was prepared by dissolving AG in the PB solution of pH 9 at 60 °C. 15% Bi-PES-SS solution was prepared by dissolving Bi-PEG-SS in the PB solution of pH 4 at room temperature. Then, 25% AG solution was mixed with 15% Bi-PEG-SS solution in equal volumes at room temperature to obtain SEAgel. SEgel was prepared using the same method as above. The prepared sealants are freeze-dried for scanning electron microscopy (SEM) observation.

**Gelation Time Measurements.** The gelation time was determined by the vial tilting method. At room temperature, 25% SEAgel solution and 15% Bi-PEG-SS solution were injected into a

**Scheme 1. Schematic Showing Fabrication and Application of SEAgel with Enhanced Cohesion Strength and Controllably Dissolvable Property<sup>a</sup>**



<sup>a</sup>By modifying gelatin with more AG, SEAgel has a denser network, potentially sealing different leakage, including bleeding and leakage in the intestine, stomach, and lung. Besides, succinic ester units are introduced into the cohesion formation. Because cysteamine can accelerate the cyclic degradation of succinic ester, endowing SEAgel with controllably dissolvable property.

vial (inner diameter 10 mm). The time at which there was no flow when inverting the vial was the gelation time.

**Compression Test.** For the compression test, the SEAgel was prepared in a cylindrical mold (diameter 10 mm, height 10 mm). Then, the compression study was carried out using a universal tension machine (CMT1103, SASCK, China). Before testing, the size of the hydrogel was measured by digital calipers. The rate of compression testing was 10 mm/min. The SEgel was used as the control. ( $n = 5$ )

**Adhesion Strength.**  $1 \times 2$  cm pigskin strips were prepared. 20  $\mu$ L of SEAgel was applied on one side of the skin, and another piece of skin was overlapped with a contact area of 1  $\text{cm}^2$ . The contact surface of the pigskin was pressed by a weight of 500 g for 10 min to minimize the thickness of the sealant, followed by a lap-shear test using a universal tension machine with a speed of 10 mm/min. ( $n = 5$ )

**Swelling Ratio and Gel Fraction.** SEgel and SEAgel with a volume of 600  $\mu$ L were prepared and put in a 10 mL centrifuge tube with PBS (pH 7.4). The tubes were kept at 37 °C overnight. Before measuring the swelling ratio (SR), excess PBS on the surface was carefully wiped off ( $n = 3$ ). The SR for the hydrogels was obtained according to the following equation

$$\text{SR}(\%) = [(W_t - W_0)/W_0] \times 100\%$$

where  $W_t$  represents the weight of the expanded hydrogel in the solution after incubation for a whole night of incubation and  $W_0$  represents the initial weight of the hydrogel before it was put into the PBS solution.

For the gel fraction test, after preparing the hydrogel, each sample was freeze-dried. The lyophilized product was carefully weighed and then put into PBS (pH 7.4) at 37 °C for 6 h. After that, the sealants were lyophilized and weighed again. The gel fraction for the hydrogels was obtained according to the following equation

$$\text{gel fraction} = (W_b/W_a) \times 100\%$$

where  $W_0$  represents the weight of the lyophilized hydrogel after being soaked and expanded in the PBS solution and  $W_a$  represents the weight of the initial lyophilization of the hydrogel. In this part, each test was repeated four times.

**Amount of Blood Absorption.** SEgel and SEAgel with a volume of 300  $\mu\text{L}$  were prepared and put in a 10 mL anticoagulation tube with 3 mL blood. The tubes were kept at 4  $^{\circ}\text{C}$  for 12 h. Before measuring the weight, excess blood on the surface was carefully wiped off ( $n = 3$ ). The amount of blood absorption for the hydrogels was obtained according to the following equation

$$\text{amount of blood absorption (g/g)} = (W_a/W_0)$$

where  $W_a$  represents the weight of the expanded hydrogel in the blood after incubation for 12 h incubation and  $W_0$  represents the initial weight of the hydrogel before it was put into the PBS solution.

**Bursting Pressure.** 3  $\times$  3 cm pigskin was used to test bursting pressure, and a hole with a diameter of 3 mm was created in the center. The sealant was applied on the surface with a syringe and set aside for 10 min to form a prototype gel with a diameter of 15 mm and a thickness of 1 mm. The pigskin was then placed on the measuring instrument. The pressure was obtained by using a syringe pump at a speed of 5 mL/min. Maximum pressure was recorded at each sealant rupture. Fibrin glue was used as the control. ( $n = 6$ )

**Torsion Experiments.** Torsion experiments were used to verify the adhesion stability of the sealant on the skin. Briefly, the SEAgel was applied in situ on the surface of the pigskin by a syringe, and then the torsional stress in different directions was applied to the pigskin to test the stability of the hydrogel on the skin.

**In Vitro Controllable Dissolution.** The hydrogel was prepared in a cylindrical mold (diameter 10 mm and height 7 mm) and then immersed in 5 mL of CA (5 wt %). Before the hydrogel was completely dissolved, the morphological size of the hydrogel and the time of complete dissolution were recorded.

**In Vitro Erasable Test.** An oval hole was created on the surface of the pigskin, and the sealant was formed in situ in the hole. A swab soaked with the CA (5% wt) solution was used to wipe the sealant.

**Cell Toxicity Tests.** NIH3T3 cells were cultured at 37  $^{\circ}\text{C}$ , 5%  $\text{CO}_2$ , and approximately  $1 \times 10^4$  cells per well were seeded in a 96-well cell culture plate. SEAgel (200 mg) was put in a fresh cell culture medium (10 mL) overnight (12 h) to obtain the leaching content (1 $\times$ ) and diluted into different concentrations (10 $\times$ , 100 $\times$ , and 1000 $\times$ ). SEAgel (1 g) was put in fresh cell culture medium (10 mL) until complete degradation to obtain degradation content and diluted into different concentrations (20, 2, 0.2, and 0.02 mg/mL). The culture medium was replaced by a series of concentrations of leaching content and degradation content diluted with the corresponding culture fluid. After 24 and 48 h, cells were washed by PBS for 3 times, 10% CCK-8 solution was added into each well, and the absorbance value of the sample solution was detected at 450 nm. Co-culture with SEAgel (5, 10, and 20 mg) is performed in a 24-well cell culture plate ( $2 \times 10^4$  cells/well), and the rest steps are the same as above.

**Liver Hemostasis Test.** All SD rats used in hepatic hemostasis tests were 100–140 g. First, the rat was deeply anesthetized and the liver lobe was exposed, filter paper was put under it. An incision (5  $\times$  3 mm) was made on the surface of the liver lobe with a scalpel blade, and blood was observed to ooze from the incision. We used a syringe to apply SEgel and SEAgel. Fibrin glue and non-treatment (Control) treatment was also tested. Before SEgel and SEAgel were applied, their precursors were pre-mixed in a single-syringe and 15 s later, SEgel and SEAgel were applied on the wounds. The starting time of the bleeding was the time when the injury was created. The bleeding time was recorded. Then, filter paper was removed and weighed, and the weight changes of the filter paper represents the different bleeding volume between the control and experimental group. After hemostasis, the liver was put back and the abdominal incision was sutured. The wounds without any treatment were used as the control. A week later, the rats were sacrificed and the liver incision was checked. The tissues were collected and H&E and Masson staining were performed. ( $n = 7$ )

**Enzyme-Linked Immunosorbent Assay for Determining Serum Antibody Responses.** The enzyme-linked immunosorbent assay (ELISA) experiments were carried out following previous reports with minor modifications.<sup>38</sup> First, SD rats (100–140 g) were immunized with SEAgel, SEgel, and Fibrin glue by applying them into the liver incisions. 7 days post-surgery, 2 mL of blood was collected from each rat. The blood was allowed to clot at 4  $^{\circ}\text{C}$  for 2 h. Then, the serum was obtained by centrifugation (2000 rpm, 4  $^{\circ}\text{C}$ , 20 min) and stored at  $-80^{\circ}\text{C}$ . Further experiments were done with those serums. To test the response, a 96-well immunoplate was coated with SEAgel, SEgel, and Fibrin glue (500 ng/mL) in 1  $\times$  bicarbonate buffer (pH 9.6) and incubated overnight at 4  $^{\circ}\text{C}$  (60  $\mu\text{L}$ /well). Rat IL-6 protein (USCN Life Science, Wuhan, China) was taken as the positive control, which also coated the plate at 500 ng/mL. Then, the plate was washed with 1  $\times$  PBS (pH 7.4) containing 0.05% Tween 20 three times with a 5 min interval. Next, the plate was incubated with 100  $\mu\text{L}$  of blocking buffer (5% BSA in wash buffer) for 3 h at room temperature followed by three times washing. Sera were serially diluted into blocking buffer from a 1:80 to 1:1280 ratio. The rabbit anti-rat IL-6 antibody (Bioss, Wuhan, China) was used as the positive control, and serial dilution was prepared as in the serum. 100  $\mu\text{L}$  of each antibody dilution was added to the corresponding coated well in triplicate and incubated at 4  $^{\circ}\text{C}$  overnight. The next day, the serum was discarded and the plate was washed three times, and then goat anti-rat IgG conjugated with HRP (Boster Co, Wuhan, China) was added to each well in 5000:1 dilution (100  $\mu\text{L}$ /well) and incubated at room temperature for 3 h. Goat anti-rabbit IgG conjugated with HRP (Boster Co, Wuhan, China) was taken as the positive control, which was also added to each well in 5000:1 dilution (100  $\mu\text{L}$ /well). After incubation, the secondary antibody was discarded, and the plate was washed three times with washing buffer. Then, 200  $\mu\text{L}$  of 1  $\times$  TMB substrate was added to each well and incubated for 2 min followed by the immediate addition of 50  $\mu\text{L}$  of 1 M  $\text{H}_2\text{SO}_4$  as the stopping solution. Finally, the absorbance value of the sample solution was detected at 450 nm.

**Real-Time Polymerase Chain Reaction.** This experiment was carried out following previous reports.<sup>38</sup> Interferon-gamma (IFN- $\gamma$ ) mRNA expression level was quantified by real-time polymerase chain reaction (PCR). SD rats with incisions were treated with PBS, SEgel, SEAgel, and Fibrin glue. Seven days later, livers from each group were collected in liquid nitrogen. Livers of untreated SD rats were taken as the control. 50 mg liver tissue was grinded and RNA were extracted using a RNAeasyTM Animal RNA Isolation Kit with Spin Column (Beyotime, China). The RNA was reverse-transcribed to obtain the cDNA using the PrimerScriptRT Master Mix (Takara, Japan). Then, the expressions of IFN- $\gamma$  mRNA were analyzed using a real-time PCR system (Biorad, America) with the SYBR Green detection method. Primers used for RT-PCR were listed as follows: IFN- $\gamma$ : (F) 5'-GGC A A A A G G A C G G T A A C A C G - 3' (R) 5'-TCTGTGGGTTGTTACCTCG-3', Actin: (F) 5'-CCC GCGAG-TACAACCTTCTT-3' (R) 5'-CCATACCCACCATCACACCC-3'. All primers were synthesized by Tsingke Biotechnology Co. Ltd (Beijing, China). All experiments are repeated three times.

**Gastric Leak Prevention Test.** The gastric tissue used for the test was taken from SD rats. One side of the stomach was sealed with sutures. A hose was inserted from the other side to connect to the syringe. A 2 mm incision was made on the surface of the stomach. Then, SEAgel was applied on the incision. Five minutes later, methylene blue solution was injected with a syringe to see whether there was a leakage. After the test, the gastric tissue coated with a hydrogel was fixed, dehydrated, and freeze-dried. SEM was further used to check the interface.

**Pulmonary Leak Prevention Test.** The gastric tissue used for the test was taken from SD rats. The intact lungs of rats were removed and the trachea was left as long as possible. An animal breathing machine was used to mimic the breathing process of rats. An incision was made on the surface of the lungs. By placing the lung tissue in water, air bubbles can be observed at the incision. Then, SEAgel was injected in situ at the incision with a syringe. Five minutes later, it was again put back into the water to see if there were still bubbles at the



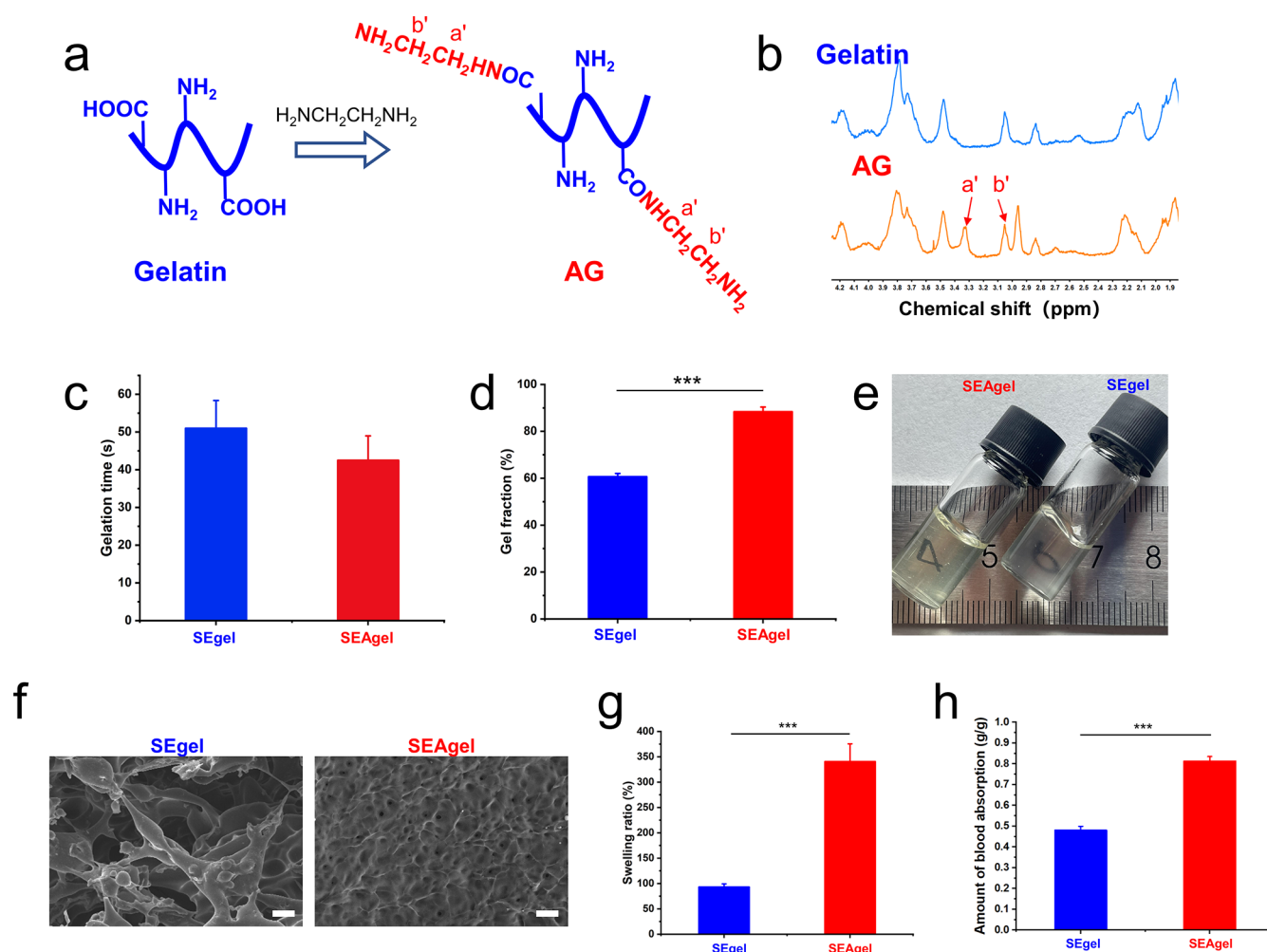


**Figure 1.** Synthesis and characterization of SEgel and SEAgel. (a,b) AG was obtained by modifying gelatin with ethanediamine (a) and NMR spectra differences between gelatin and AG were presented (b). (c) Gelation time of SEgel and SEAgel. (d) Gel fraction of SEgel and SEAgel. (e) Picture showing that SEAgel was more transparent than SEgel. (f) SEM results of SEgel and SEAgel (scale bar = 20  $\mu\text{m}$ ). (g) SR of SEgel and SEAgel. (h) Blood absorption ability of SEgel and SEAgel.

incision site. After the test, the part of the gel that adhered to the tissue was fixed, dehydrated, and freeze-dried. SEM was further used to check the interface.

**Intestine Antileakage Test.** The intestine was obtained from a New Zealand white rabbit. One side of the large intestine was closed with sutures and the other side was connected to a syringe. A 2 mm incision was made on the surface of the intestine to create the leakage. SEAgel was applied in situ on the incision. 5 min later, methylene blue solution was injected into the large intestine and the leakage was checked. After the test, SEM was further used to check the interface.

**Cephalic Artery Hemostasis Test.** The New Zealand white rabbit was used to build a massive hemorrhage model. After the rabbit was anesthetized, the cephalic artery was exposed and punctured with a 23G needle. After wiping the blood on the surface by gauze, in different rabbit surgeries, the SEAgel, SEgel, and Fibrin glue was injected in situ at the puncture site immediately. We checked whether the bleeding site was blocked and if there was still bleeding after 5 min. Ten minutes later, the wounds were sutured, and the vital signs of the rabbit were observed. After 7 days, the rabbit was sacrificed, the artery was checked, collected, fixed, and H&E and Masson staining procedures were carried out.

**Heart Bleeding Experiments.** The bleeding was caused by 18G needle with high-pressure blood expulsion. When the needle was removed, bleeding was still observed. Then, SEAgel was applied on the blood hole and the bleeding was visually checked.

**Statistical Analysis.** The data are presented as means  $\pm$  standard deviation (SD). The statistical analyses between different groups were determined with Student's *t*-tests. A value of  $p < 0.05$  was considered as statistically significantly different (\* $p < 0.05$ , \*\* $p < 0.01$ , \*\*\* $p < 0.001$ ).

**Ethics.** All the animal studies were carried out in accordance with Xi'an Jiaotong University Ethics Committee on the use of Animals in Research and Teaching.

## RESULTS AND DISCUSSION

First of all, AG was obtained by modifying gelatin with ethanediamine following the reported procedures.<sup>37</sup> After modification, the nuclear magnetic resonance (NMR) test showed two new peaks at 3.3 and 3.05 ppm belonging to the  $\text{CH}_2$  groups of succinic units, proving that ethanediamine was successfully grafted to the main gelatin chain (Figure 1a,b). Then, AG was mixed with Bi-PEG-SS to form the sealant SEAgel with succinic ester units as the controllably dissolvable part. The gelatin without modification was also mixed with Bi-PEG-SS as the control (SEgel). The gelation time for SEgel was  $51.0 \pm 7.3$  s, while it was  $42.5 \pm 6.4$  s for SEAgel (Figure 1c). A higher gelation speed was observed for SEAgel because the content of reactive functional groups increased.



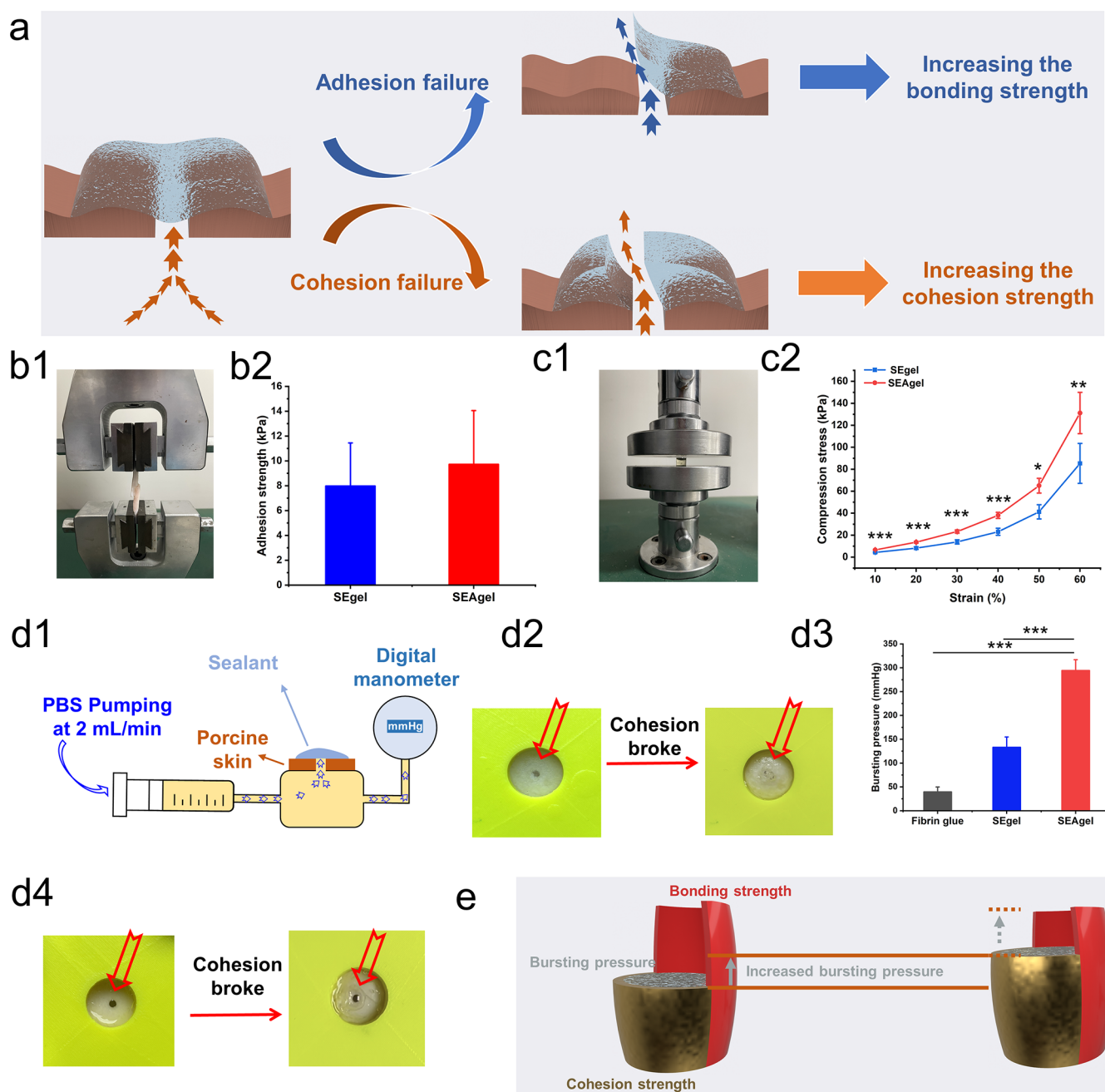


**Figure 2.** Bursting performance of SEgel and SEAgel. (a) Schematic showing two ways of bursting after the sealing. The first one is the adhesion failure, in which case increasing the bonding strength will increase the bursting pressure. The second one is the cohesion failure, in which case increasing the bulk strength will increase the bursting pressure. (b) Picture (b1) and result (b2) of the lap shear test. (c) Picture (c1) and result (c2) of the compression study. (d) Bursting pressure test. (d1) Schematic showing the bursting pressure testing. (d2) Picture showing that cohesion broke for SEgel during the bursting pressure test. (d3) Bursting pressure test result. (d4) Picture showing that cohesion broke for SEAgel during the bursting pressure test. (e) Schematic showing the bursting pressure is related to both cohesion and adhesion.

After modification, the cross-linking density was supposed to be higher, leading to a more integral network. To verify that, the gel fraction test was carried out. The gel fraction is defined as the weight ratio of the dried network polymer to that of the polymer before being washed by the solvent. Figure 1d shows that SEAgel had a gel fraction of  $88.4 \pm 2.0\%$ , significantly larger than that of SEgel  $60.7 \pm 1.3\%$ . A more significant gel fraction means that SEAgel has a more intact network, contributing to a strong cohesion strength. It was also surprising to find that SEAgel formed with a more transparent gel state, demonstrating a more homogeneous network

structure, which is suitable for achieving a solid cohesion strength (Figure 1e).<sup>39</sup> The denser network was further proved by the SEM images, showing that SEgel has a loose porous structure with an irregular pore size (Figure 1f). However, for SEAgel, SEM demonstrated a denser network and more uniform system. It was also observed in SEM that SEAgel showed a thinner and more consistent texture while that for SEgel was thicker with nonuniformity, which might explain why the SEAgel was more transparent when compared with SEgel.<sup>39,40</sup> The swelling test was later carried out, illustrating that SEAgel ( $340.6 \pm 34.9\%$ ) expressed a significantly larger

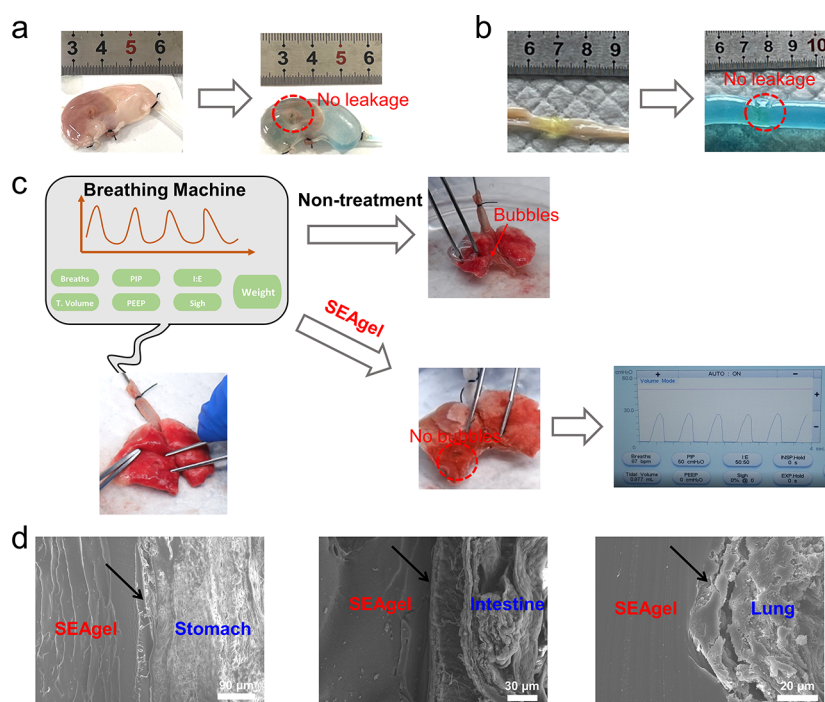


**Figure 3.** Results of using SEAgel to seal the stomach, intestine, and lung. (a) SEAgel sealed leakage of the rat stomach. (b) SEAgel sealed leakage of the rabbit intestine. (c) SEAgel sealed the leakage of the rat lung. When the lung was connected to a breath machine and immersed in water, there were no bubbles observed for SEAgel and the pressure reading on the screen did not decrease during the test. Those incisions were 2 mm in length. (d) SEM images showing the interface between SEAgel and different tissues, including the stomach, intestine, and lung.

SR than that of SEgel ( $93.2 \pm 6.0\%$ ) (Figure 1g). We deduce this happened because the electrostatic attraction between amino groups and carboxyl groups (SEgel) changed into electrostatic repulsion after the modification, leading to a bigger swelling of SEAgel. For sealants, a big SR is sometimes needed to absorb more tissue fluids to help concentrate the blood coagulation factor or do good nutrient exchange and metabolic waste transfer.<sup>34</sup> Figure 1h shows that within the same time, SEAgel absorbed more blood when compared with SEgel, showing its advantages in hemostasis. However, the large SR might press the surrounding brittle tissues, thus limiting the applications of SEAgel in some sensitive tissues, like nerves, and so forth.

The bursting pressure is the decisive feature for sealants, and the overall sealing behavior is decided by the adhesion strength, which is the bonding between tissues and sealants, and cohesion strength which is the bulk strength of the sealants.<sup>34,41</sup> It is preferred that the larger the bursting pressure is, the better its sealing efficacy is. After sealing, there are two basic ways for leakage (Figure 2a). One is the breakage of the adhesion area between sealants and tissues, meaning the adhesion failure. In this case, increasing the bonding strength will improve the bursting pressure performance. The second breakage is the bulk breakage, indicating the cohesion failure. In this case, increasing the cohesion strength will lead to a higher bursting pressure. To demonstrate the adhesion strength and cohesion strength, lap shear and compression tests were carried out. First, the lap shear tests were designed following ASTM F2255-05. We pressed the testing strip hard after overlapping two tissue strips to minimize the cohesion influence on the testing. It was hypothesized that in this situation, the adhesion strength indicates the bonding strength between sealants and tissues. It was found in Figure 2b that SEgel and SEAgel showed similar adhesion strength without

significant difference ( $8.0 \pm 3.5$  kPa for SEgel and  $9.7 \pm 4.3$  kPa for SEAgel). The adhesion performance was mainly ascribed to the reaction between the NHS-ester and AGs from tissue proteins. Similar adhesion strength proves that modification did not affect the bonding strength between tissues and the sealants. However, the compression test illustrated that at a similar strain, the mechanical strength for SEAgel significantly increased compared with that of SEgel, showing a significantly increased cohesion strength (Figure 2c). Later, the bursting pressure test was carried out following ASTM F2392-04 (Figure 2d1). For SEgel, the bursting happened at the center, showing that SEgel underwent cohesion failure during the test (Figure 2a,d2). Therefore, according to the discussion, it was hypothesized here that increasing the cohesion strength would lead to a higher bursting pressure. Figure 2d3 shows that the average bursting pressure was  $133.2 \pm 21.4$  mmHg for SEgel, and it reached  $294.3 \pm 22.5$  mmHg for SEAgel, while the commercialized Fibrin glue had a bursting pressure of  $39.5 \pm 10.4$  mmHg. The results illustrated that the cohesion increase indeed improves the sealing performance. In fact, for SEAgel, the bursting still happened at the center of the gel, proving that even for SEAgel, it underwent cohesion failure (Figure 2a,d4). As discussed before, in this situation, increasing the cohesion strength will still improve the final bursting performance. To better visualize the whole concept of our design, the entire process was simplified by using the Cannikin Law (Figure 2e). The adhesion strength and cohesion strength may be the two halves of the buckets deciding the amount of inside “water”, which is bursting pressure here. After modification, the cohesion strength significantly increased, leading to an increased bursting pressure. However, it was shown in our experiments that for SEAgel, the cohesion still broke first during the process, proving that further expansion of the

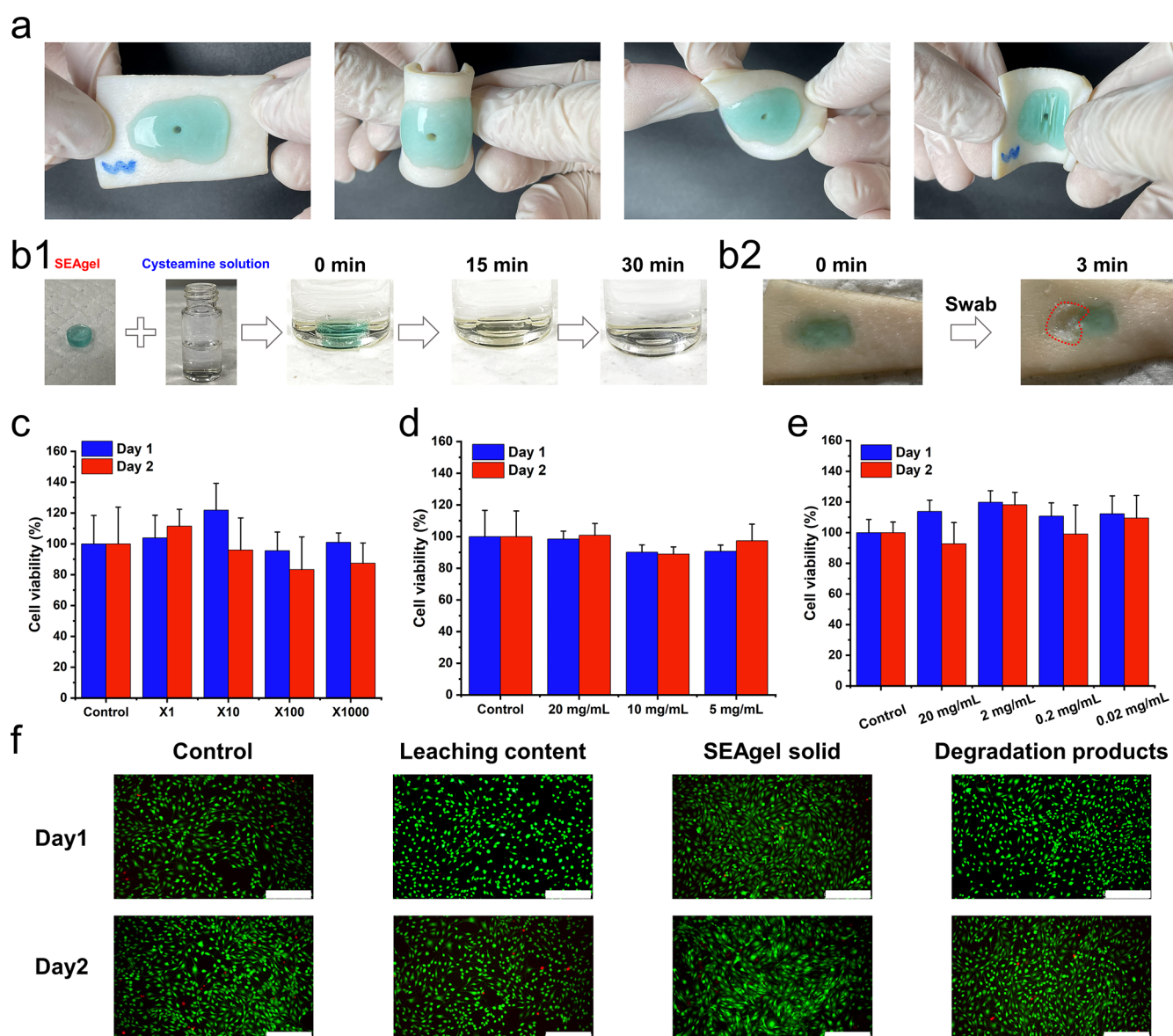


**Figure 4.** Controllably removable property and cytocompatibility of SEAgel. (a) SEAgel kept stable under different torsion. (b1) Dissolution of SEAgel in 5% CA. (b2) Removal of SEAgel using a cysteamine-soaked swab. (c–e) Cell viability result of NIH3T3 cells when co-cultured with leaching content of SEAgel, SEAgel solid, and degradation products of SEAgel. (f) Live&Dead assay results of NIH3T3 when co-cultured with leaching content, SEAgel solid, and degradation products (scale bar = 250  $\mu$ m,  $n = 6$ ).

cohesion strength may further enhance the bursting pressure performance of this system.

To illustrate the universality of this sealant, incisions (2 mm in length) on the rat stomach, rabbit intestine, and rat lung were made and SEAgel was then applied. It was shown in Figure 3a,b that after using SEAgel, no methylene blue solution came out of the defects when the injection happened. For rat lung sealing, a breathing machine was connected to the lung through its respiratory tract. It was found without sealing, there were a lot of bubbles coming out of the defects when immersing the lung in the water (Figure 3c). However, after closing with SEAgel, no bubbles came out, and the reading on the breathing machine was kept stable at around 24 cm H<sub>2</sub>O, showing a good sealing effect (Figure 3c). Further, SEM was applied to analyze the ultrastructural appearance of the surface of the sealant's adhesion to different tissues. Figure 3d shows a closed and effective sealing appearance between SEAgel and

various tissues, confirming the tight bonding and successful sealing.

Another charming property of modern sealants is the easy removability in the case of second exposure for wound care or the need to be removed if the sealing fails. This is especially true when the operation happens in elders who have more brittle organs and a weakened healing ability. Cohesion strategies were reported to endow bioadhesives with different functions, like easy removability, self-healing, and even other biological functions like antibacterial and antioxidant.<sup>19,36,42,43</sup> Hence, in our work, to endow the bioadhesives with controllable dissolution properties, succinyl ester was introduced. This unit was formed by using succinic anhydride-modified Bi-PEG–SS. It was proven in our previous work that succinyl ester processed a cyclic degradation behavior with good controllability by using CA, which is an FDA-approved drug.<sup>20</sup> In this work, SEAgel with succinyl ester also showed controllable dissolution properties. Figure 4a shows that



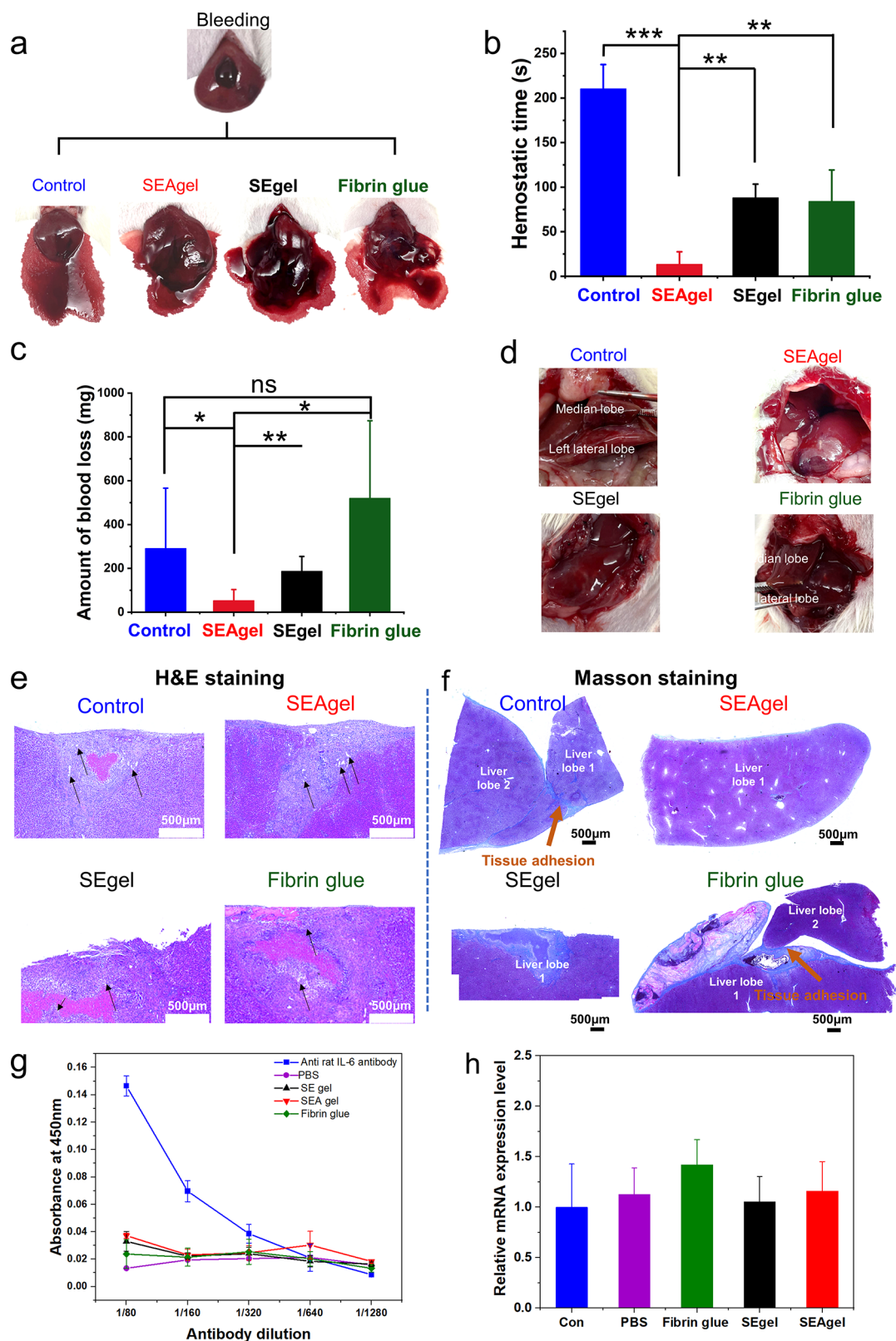


**Figure 5.** SEAgel efficiently stopped the bleeding in the rat liver incision model. (a) Pictures showing the hemostasis experiments using SEAgel, SEgel, and Fibrin glue. The bleeding livers without any treatment were used as the control. (b,c) Hemostatic time (b) and amount of blood loss (c) during the tests. (d) Pictures show that 7 days post-surgery, there was liver adhesion between different liver lobes for the control and Fibrin glue-treated groups. (e) H&E staining of wounds 7 days post-surgery. The black arrow indicates the bile ducts. (f) Masson staining of liver lobes 7 days post-surgery. (g) Serum IgG response of rats after 7 days post-immunization by ELISA. (h) Real-time PCR result showing the IFN- $\gamma$  cytokine gene expression after the liver was treated with nothing (control), PBS, Fibrin glue, SEgel, and SEAgel.

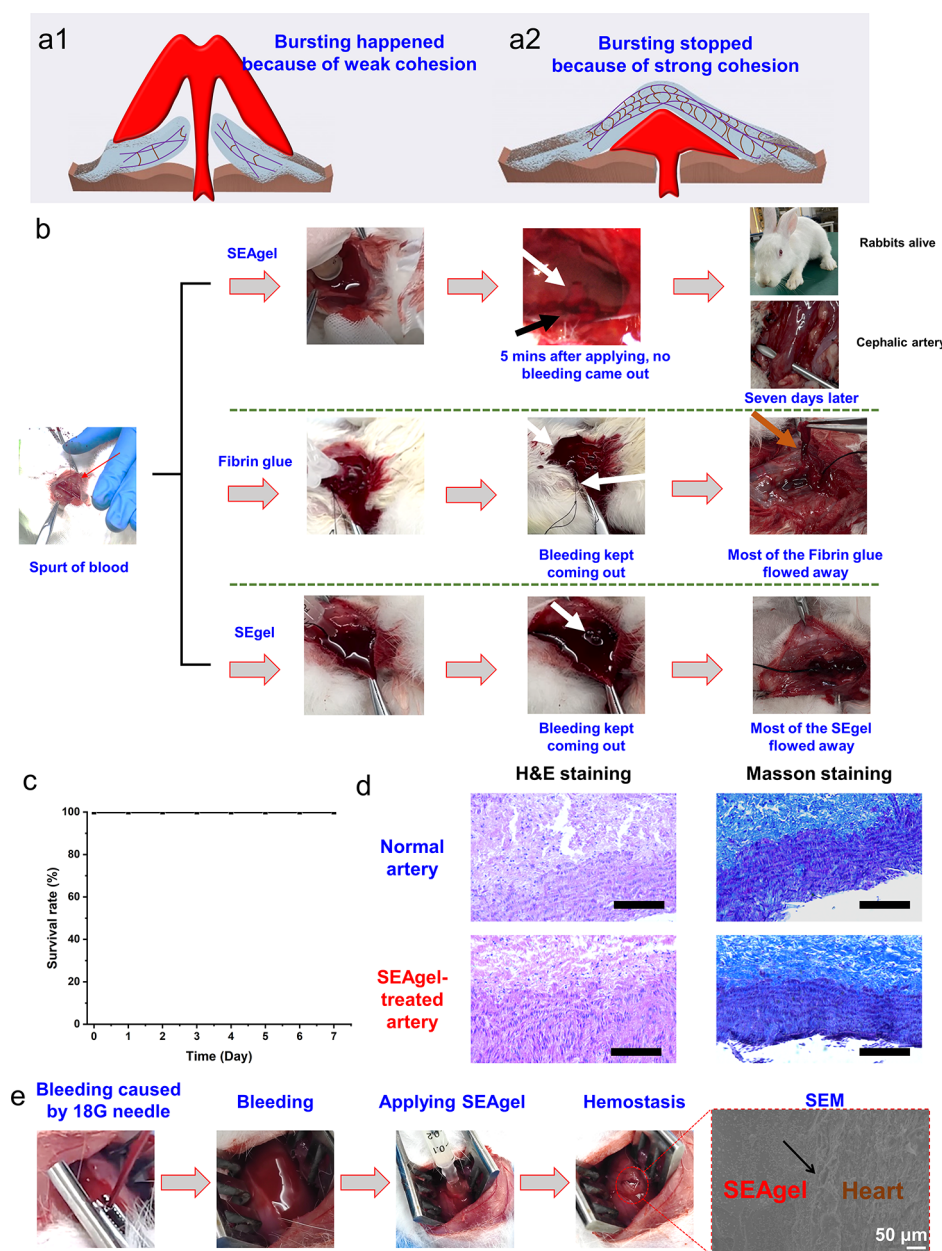


**Figure 6.** SEAgel efficiently stopped the bleeding in the rabbit cephalic artery injury model. (a) Schematic showing that weak cohesion easily leads to bursting, limiting the use in active bleeding. However, a high cohesion can stop the bursting efficiently. (b) Pictures showing the process of the cephalic artery injury model. A 23G needle was used to penetrate the cephalic artery to create a blood spurt. Instead of using forceps to control the bleeding, gauze was used to remove the surrounding blood after which SEAgel was applied immediately. Right after application, no blood came out. Seven days later, the rabbits were found alive ( $n = 3$ ). In contrast, SEgel and Fibrin glue were washed away and could not stop the bleeding, with the blood continuously coming out of the vessels. (c) Survival rate of the SEAgel-treated rabbits in the cephalic artery injury model during the first seven days post-surgery. (d) H&E and Masson staining result of SEAgel-treated cephalic artery compared with the normal cephalic artery (scale bar = 200  $\mu\text{m}$ ). (e) Gross view of the rapid sealing of SEAgel after cardiac puncture injury. The bleeding was caused by a 18G needle with high-pressure blood expulsion. When the needle was removed, bleeding was still observed. Then, SEAgel was applied on the blood hole and the bleeding stopped immediately. SEM showed that SEAgel firmly adhered to the cardiac tissues.

SEAgel became a transparent state after being applied to the porcine skin and kept stable under different torsions, demonstrating its stability. However, after immersing SEAgel in 5% CA, it dissolved in less than 30 min, showing that CA could remove SEAgel (Figure 4b1). Later, a cysteamine-soaked swab was used to remove SEAgel in the hole of porcine skin in 3 min (Figure 4b2). These results indicate that SEAgel could be controllably removed, which is useful when the re-exposure of wounds is needed.

Safety is one of the most critical factors in deciding if a biomaterial can be used or not, and a sealant must process good biocompatibility for in vivo applications. Here, two components of our system were amine-modified gelatin and Bi-PEG-SS. It was shown previously that bioadhesives fabricated by gelatin and Bi-PEG-SS were biocompatible.<sup>33</sup> Here, to further illustrate that modification of gelatin did not cause any cytotoxicity, three cell culture experiments were carried out, including co-culture of NIH3T3 cells with the

leaching content (Figure 4c), SEAgel solid (Figure 4d), and the degradation products (Figure 4e). According to ISO standards, the biomaterials are not toxic if the cell viability is more than 70%.<sup>44</sup> It was shown in Figure 4 that all the cell viability was more than 70% at the chosen concentrations, proving the excellent cytocompatibility of SEAgel. Further, the Live&Dead assays also demonstrated that very few dead cells could be observed during the cytotoxicity studies (Figure 4f), again demonstrating the good cytocompatibility of SEAgel.

To illustrate the *in vivo* sealing ability of this sealant, two animal models, including a rat liver bleeding model and a rabbit cephalic artery injury model, were used. In the rat liver bleeding model, wounds with a length of 5 mm and a depth of 3 mm were made with the surgical blades (Figure 5a). It was shown that without any treatment the bleeding continued even after 200 s, with an average bleeding time of  $210 \pm 22$  s. However, after applying SEAgel, SEgel and Fibrin glue, the bleeding time decreased (Figure 5b). For SEAgel, it has the significantly shortest bleeding time as  $13 \pm 14$  s among all the groups ( $88 \pm 15$  s for SEgel-treated and  $84 \pm 35$  s for Fibrin glue-treated), showing its ability to efficiently seal the bleeding. Meanwhile, the amount of the bleeding was also the least among the four groups ( $291 \pm 274$  mg for the control,  $53 \pm 50$  mg for SEAgel-treated,  $187 \pm 67$  mg for SEgel-treated, and  $520 \pm 354$  mg for Fibrin glue-treated), further demonstrating the efficacy of this material in stopping bleeding (Figure 5c). It was worth noting that three of seven SEAgel-treated animals stopped bleeding immediately with no blood leaking. In our experiments, although Fibrin glue decreased the bleeding time, it did not decrease the amount of blood loss (Figure 5c). This happened because when the Fibrin glue was applied on the bleeding wounds, it flowed to the filter paper resulting from the bleeding flow, leading to a high weight value. Seven days after the surgery, all the animals were sacrificed, and the livers were visually checked (Figure 5d,e). Figure 5d shows that for control groups without any treatment, some of the unoperated liver lobes adhered to the wounded lobes, which was impossible to separate them without impairing the livers. It was deduced that the liver lobe adhesion might be caused by the physical contact between the wounded area and healthy tissues, which is a common post-operative complication.<sup>45</sup> However, for SEgel/SEAgel-treated livers, few liver lobe adhesions were observed while six out of seven Fibrin glue-treated animals showed liver lobe adhesions. Later, the H&E staining in Figure 5f shows that the wound started healing for all the livers, with newly regenerated bile ducts observed. However, Masson staining showed in the control and Fibrin glue-treated groups, there was severe fibroplasia connecting different liver lobes, while it was seldom observed for SEgel/SEAgel-treated groups (Figure 5g). Altogether, these data proved that SEAgel can not only efficiently stopped the bleeding but also may prevent the liver adhesion after surgery. To further prove the safety of the SEAgel, immunogenic response experiments were carried out following the previous report.<sup>38</sup> The ELISA results showed that a very low IgG response was observed for SEAgel, which was not significantly different when compared to that of the commercially available Fibrin glue (Figure 5g). The pro-inflammatory cytokine IFN- $\gamma$  was also detected showing that SEAgel did not induce the over-expression of the cytokine, further demonstrating the good biocompatibility of SEAgel (Figure 5f). In the future, the immunogenic response can be further optimized by using gelatin of medical grade.

A big problem for traditional injectable sealants in sealing the bleeding of blood vessels is that the blood flow with high pressure might easily wash away the precursor solution before the sealants can form a stable barrier. Therefore, it is a routine procedure that the blood vessels are closed by the forceps to stop the active bleeding, and then the sealants are applied.<sup>18,32,46</sup> One of the reasons is that those sealants cannot form an immediate strong cohesion (Figure 6a). In our system, it was hypothesized that SEAgel might be able to withstand the high pressure generated by the blood flow because of the high cohesion strength (Figure 6a). To show that, a small hole was created in the carotid artery using a 23G needle, after which a spurt of blood was observed (Figure 6b). Without using the forceps, a gauze was used to absorb the surrounding blood, after which immediately SEAgel was applied. The blood was completely sealed around the blood vessels, and no more bleeding was observed (Figure 6b). It was also observed that a blood clot (white arrow) is observed in Figure 6b, just like the situation in Figure 6a2. It proved that although there was some blood coming out of the vessels, SEAgel still successfully sealed the active bleeding because of high cohesion strength. In contrast, there was still blood coming out of the vessels treated with Fibrin glue and SEgel (Figure 6b). Those animals treated with SEgel and Fibrin glue were sacrificed because of unstoppable bleeding. There was only a little residual SE gel and Fibrin glue observed because most of it flowed away under the high blood pressure (Figure 6b). All the SEAgel-treated rabbits were found alive post-surgery with 100% survival rate (Figure 6c). Seven days later, the rabbits were anesthetized, and the carotid artery was exposed. The carotid artery showed good beating behavior with little inflammation observed, further demonstrating the good biocompatibility of SEAgel (Figure 6b). No residual materials could be observed because of the fast degradable properties of the succinic ester-based bioadhesives.<sup>20,33</sup> Further, H&E and Masson staining were carried out and demonstrated that SEAgel did not cause any side effects, further illustrating the good biocompatibility of the sealant (Figure 6d). Further, the sealing ability of this sealant was demonstrated by using a rabbit cardiac puncture model. Figure 6e shows that after using an 18 G needle to penetrate the heart wall, blood expulsion was observed. The bleeding continued after removing the needle. Immediately after applying SEAgel, the bleeding stopped, illustrating that SEAgel efficiently sealed the defect. After the experiments, it was found that SEAgel firmly adhered to the heart tissues by SEM. All together, these results showed that SEAgel had a good sealing effect even with active bleeding.

## CONCLUSIONS

In summary, by a cohesion strategy design, we fabricated a sealant with intense bursting pressure and controllably removable properties. The bursting pressure was enhanced by increasing the cross-linking density of the sealant and the smartly removable property was achieved by using the succinic ester units. Both the *in vivo* and *in vitro* experiments showed that this sealant presented a good sealing ability to different organs with good biocompatibility, which is quite promising for commercialization. However, considering that this sealant disappeared seven days after implantation, it is unsuitable for sealing those wounds that need long periods of sealing. However, considering the good biocompatibility, SEAgel is quite suitable for some extremely important organs with low tolerance to the materials-induced inflammation, like repro-



duction-related ones. Also, all the animal studies were carried out in small animals, and experiments in large animals are still needed to test its efficacy in the future.

## AUTHOR INFORMATION

### Corresponding Authors

**Zuquan Weng** — College of Biological Science and Engineering, Fuzhou University, Fuzhou, Fujian 350108, China; [orcid.org/0000-0002-1089-8673](https://orcid.org/0000-0002-1089-8673); Email: [wengzq@fzu.edu.cn](mailto:wengzq@fzu.edu.cn)

**Yuan Zhu** — Department of Gynecology, The Affiliated Maternal and Child Healthcare Hospital of Nanchang University, Nanchang, Jiangxi 330006, China; Department of Gynecology, Jiangxi Provincial Maternal and Child Health Hospital, Nanchang, Jiangxi 330006, China; Email: [zhuyuan0528@aliyun.com](mailto:zhuyuan0528@aliyun.com)

**Yazhong Bu** — Institute of Medical Engineering, Department of Biophysics, School of Basic Medical Sciences, Health Science Center, Xi'an Jiaotong University, Xi'an 710061, China; Key Laboratory of Environment and Genes Related to Diseases (Xi'an Jiaotong University), Ministry of Education of China, Xi'an 710061, China; [orcid.org/0000-0003-0987-8453](https://orcid.org/0000-0003-0987-8453); Email: [yazhongbu@xjtu.edu.cn](mailto:yazhongbu@xjtu.edu.cn)

### Authors

**Chaowei Li** — College of Biological Science and Engineering, Fuzhou University, Fuzhou, Fujian 350108, China; Institute of Medical Engineering, Department of Biophysics, School of Basic Medical Sciences, Health Science Center, Xi'an Jiaotong University, Xi'an 710061, China

**Wanglin Duan** — Institute of Medical Engineering, Department of Biophysics, School of Basic Medical Sciences, Health Science Center, Xi'an Jiaotong University, Xi'an 710061, China

**Ye Zhu** — Institute of Medical Engineering, Department of Biophysics, School of Basic Medical Sciences, Health Science Center, Xi'an Jiaotong University, Xi'an 710061, China

**Guanying Li** — Institute of Medical Engineering, Department of Biophysics, School of Basic Medical Sciences, Health Science Center, Xi'an Jiaotong University, Xi'an 710061, China; Key Laboratory of Environment and Genes Related to Diseases (Xi'an Jiaotong University), Ministry of Education of China, Xi'an 710061, China

**Min Gao** — Institute of Molecular and Translational Medicine, Department of Biochemistry and Molecular Biology, School of Basic Medical Sciences, Xi'an Jiaotong University, Xi'an 710061, China

Complete contact information is available at: <https://pubs.acs.org/10.1021/acsami.2c08328>

### Author Contributions

The manuscript was written through contributions of all authors. All authors have given approval to the final version of the manuscript. C.L. and W.D. contributed equally to this paper.

### Funding

This work was supported by the National Natural Science Foundation of China (grant nos. 52103184, 81971837, and 81660265), the Natural Science Foundation of Jiangxi Province (grant no. 20181BAB205015), Key Research and Development Program of Jiangxi Province (grant no. 20202BBGL73065), and "Young Talent Support Plan" of Xi'an Jiaotong University.

## Notes

The authors declare no competing financial interest.

## ACKNOWLEDGMENTS

We sincerely thank Hongwen Yu, Prof. Baoji Du, Prof. Fuquan Huo and Prof. Yilei Zhang from Xi'an Jiaotong University for offering practical advice in this work. Figure <sup>1</sup> and TOC were created with the help of [BioRender.com](https://www.biorender.com).

## REFERENCES

- (1) Hummel, R.; Bausch, D. Anastomotic Leakage after Upper Gastrointestinal Surgery: Surgical Treatment. *Visc. Med* **2017**, *33*, 207.
- (2) Spence, R. T.; Hirpara, D. H.; Doshi, S.; Queresby, F. A.; Chadi, S. A. Anastomotic Leak after Colorectal Surgery: Does Timing affect Failure to Rescue? *Surg. Endosc.* **2022**, *36*, 771.
- (3) Mizuta, R.; Taguchi, T. Hemostatic Properties of in Situ Gels Composed of Hydrophobically Modified Biopolymers. *J. Biomater. Appl.* **2018**, *33*, 315.
- (4) Erfani, H.; Salmanian, B.; Fox, K. A.; Coburn, M.; Meshinchiasl, N.; Shamshirsaz, A. A.; Kopkin, R.; Gogia, S.; Patel, K.; Jackson, J.; Cadena, M.; Aalipour, S.; Sukumar, S.; Nassr, A. A.; Espinoza, J.; Clark, S. L.; Belfort, M. A.; Shamshirsaz, A. A. Urologic Morbidity Associated with Placenta Accreta Spectrum Surgeries: Single-Center Experience with A Multidisciplinary Team. *Am. J. Obstet. Gynecol.* **2022**, *226*, 245.
- (5) Majd, H. S.; Collins, S. L.; Addley, S.; Weeks, E.; Chakravarti, S.; Halder, S.; Alazzam, M. The Modified Radical Peripartum Cesarean Hysterectomy (Soleymani-Alazzam-Collins Technique): A Systematic, Safe Procedure for The Management of Severe Placenta Accreta Spectrum. *Am. J. Obstet. Gynecol.* **2021**, *225*, 175.
- (6) Mueller, M. R.; Marzluf, B. A. The Anticipation and Management of Air Leaks and Residual Spaces Post Lung Resection. *J. Thorac. Dis.* **2014**, *6*, 271.
- (7) Duan, W.; Bian, X.; Bu, Y. Applications of Bioadhesives: A Mini Review. *Front. Bioeng. Biotechnol.* **2021**, *9*, 716035.
- (8) Tavafooghi, M.; Sheikhi, A.; Tutar, R.; Jahangiry, J.; Baidya, A.; Haghniaz, R.; Khademhosseini, A. Engineering Tough, Injectable, Naturally Derived, Bioadhesive Composite Hydrogels. *Adv. Healthcare Mater.* **2020**, *9*, 1901722.
- (9) Hennis, H. L.; Stewart, W. C.; Jeter, E. K. Infectious Disease Risks of Fibrin Glue. *Ophthalmic Surg. Lasers Imaging Retina* **1992**, *23*, 640.
- (10) Saffarzadeh, M.; Mulpuri, A.; Arneja, J. S. Recalcitrant Anaphylaxis Associated with Fibrin Sealant: Treatment with "TISSEEL-Ectomy". *Plast. Reconstr. Surg.-Glob.* **2021**, *9*, No. e3382.
- (11) Kanazawa, R.; Sato, S.; Iwamoto, N.; Teramoto, A. Allergic Reaction Following Arachnoid Plasty with A Fibrin Sealant. *Neurol. Med.-Chir.* **2010**, *50*, 608.
- (12) Spotnitz, W. D.; Burks, S. Hemostats, Sealants, and Adhesives: Components of The Surgical Toolbox. *Transfusion* **2008**, *48*, 1502.
- (13) Burks, S.; Spotnitz, W. Safety and Usability of Hemostats, Sealants, and Adhesives. *AORN J.* **2014**, *100*, 160.
- (14) Spotnitz, W. D.; Burks, S. Hemostats, Sealants, and Adhesives III: A New Update as well as Cost and Regulatory Considerations for Components of The Surgical Toolbox. *Transfusion* **2012**, *52*, 2243.
- (15) Vyas, K. S.; Saha, S. P. Comparison of Hemostatic Agents Used in Vascular Surgery. *Expet Opin. Biol. Ther.* **2013**, *13*, 1663.
- (16) Luk, A.; David, T. E.; Butany, J. Complications of Biogluce Postsurgery for Aortic Dissections and Aortic Valve Replacement. *J. Clin. Pathol.* **2012**, *65*, 1008.
- (17) LeMaire, S. A.; Ochoa, L. N.; Conklin, L. D.; Schmittling, Z. C.; Ündar, A.; Clubb, F. J.; Li Wang, X.; Coselli, J. S.; Fraser, C. D. Nerve and Conduction Tissue Injury Caused by Contact with BioGlue. *J. Surg. Res.* **2007**, *143*, 286.
- (18) Bhamidipati, C. M.; Coselli, J. S.; LeMaire, S. A. BioGlue in 2011: What is Its Role in Cardiac Surgery? *J. Extra Corpor. Technol.* **2012**, *44*, 6.

- (19) Zhao, X.; Liang, Y.; Huang, Y.; He, J.; Han, Y.; Guo, B. Physical Double-Network Hydrogel Adhesives with Rapid Shape Adaptability, Fast Self-Healing, Antioxidant and NIR/pH Stimulus-Responsiveness for Multidrug-Resistant Bacterial Infection and Removable Wound Dressing. *Adv. Funct. Mater.* **2020**, *30*, 1910748.
- (20) Bu, Y.; Zhang, L.; Sun, G.; Sun, F.; Liu, J.; Yang, F.; Tang, P.; Wu, D. Tetra-PEG Based Hydrogel Sealants for in Vivo Visceral Hemostasis. *Adv. Mater.* **2019**, *31*, 1901580.
- (21) Gowda, A. H. J.; Bu, Y.; Kudina, O.; Krishna, K. V.; Bohara, R. A.; Eglon, D.; Pandit, A. Design of Tunable Gelatin-Dopamine Based Bioadhesives. *Int. J. Biol. Macromol.* **2020**, *164*, 1384.
- (22) Gorgieva, S.; Kokol, V. Collagen-VS. Gelatine-Based Biomaterials and Their Biocompatibility: Review And Perspectives. *Biomater. Appl. Nanomed.* **2011**, *2*, 17.
- (23) Sharifi, S.; Islam, M. M.; Sharifi, H.; Islam, R.; Koza, D.; Reyes-Ortega, F.; Alba-Molina, D.; Nilsson, P. H.; Dohlmann, C. H.; Mollnes, T. E.; Chodosh, J.; Gonzalez-Andrades, M. Tuning Gelatin-Based Hydrogel Towards Bioadhesive Ocular Tissue Engineering Applications. *Bioact. Mater.* **2021**, *6*, 3947.
- (24) Park, H.; Temenoff, J. S.; Holland, T. A.; Tabata, Y.; Mikos, A. G. Delivery of TGF- $\beta$ 1 and Chondrocytes via Injectable, Biodegradable Hydrogels for Cartilage Tissue Engineering Applications. *Biomaterials* **2005**, *26*, 7095.
- (25) Nomori, H.; Horio, H.; Morinaga, S.; Suemasu, K. Gelatin-Resorcinol-Formaldehyde-Glutaraldehyde Glue for Sealing Pulmonary Air Leaks During Thoracoscopic Operation. *Ann. Thorac. Surg.* **1999**, *67*, 212.
- (26) Zhang, Y.; Wang, Q. S.; Yan, K.; Qi, Y.; Wang, G. F.; Cui, Y. L. Preparation, Characterization, and Evaluation of Genipin Crosslinked Chitosan/Gelatin Three-Dimensional Scaffolds for Liver Tissue Engineering Applications. *J. Biomed. Mater. Res.* **2016**, *104*, 1863.
- (27) Kirchmayer, D. M.; Watson, C. A.; Ranson, M.; Panhuis, M. Gelatin, A Degradable Genipin Cross-Linked Gelatin Hydrogel. *RSC Adv.* **2013**, *3*, 1073.
- (28) Suzuki, S.; Ikada, Y. Sealing Effects of Cross-Linked Gelatin. *J. Biomater. Appl.* **2012**, *27*, 801.
- (29) Mizuta, R.; Ito, T.; Taguchi, T. Effect of Alkyl Chain Length on The Interfacial Strength of Surgical Sealants Composed of Hydrophobically-Modified Alaska-Pollock-Derived Gelatins and Poly-(ethylene)glycol-Based Four-Armed Crosslinker. *Colloids Surf., B* **2016**, *146*, 212.
- (30) Taguchi, T.; Mizuta, R.; Ito, T.; Yoshizawa, K.; Kajiyama, M. Robust Sealing of Blood Vessels with Cholesteryl Group-Modified, Alaska Pollock-Derived Gelatin-Based Biodegradable Sealant Under Wet Conditions. *J. Biomed. Nanotechnol.* **2016**, *12*, 128.
- (31) Li, X.; Tsutsui, Y.; Matsunaga, T.; Shibayama, M.; Chung, U.-i.; Sakai, T. Precise Control and Prediction of Hydrogel Degradation Behavior. *Macromolecules* **2011**, *44*, 3567.
- (32) Bu, Y.; Zhang, L.; Liu, J.; Zhang, L.; Li, T.; Shen, H.; Wang, X.; Yang, F.; Tang, P.; Wu, D. Synthesis and Properties of Hemostatic and Bacteria-Responsive in Situ Hydrogels for Emergency Treatment in Critical Situations. *ACS Appl. Mater. Interfaces* **2016**, *8*, 12674.
- (33) Wang, P.; Zhu, Y.; Feng, L.; Wang, Y.; Bu, Y. Rapidly Self-Deactivating and Injectable Succinyl Ester-Based Bioadhesives for Postoperative Antiadhesion. *ACS Appl. Mater. Interfaces* **2022**, *14*, 373.
- (34) Bu, Y.; Pandit, A. Cohesion Mechanisms for Bioadhesives. *Bioact. Mater.* **2022**, *13*, 105.
- (35) Lu, H.; Yuan, L.; Yu, X.; Wu, C.; He, D.; Deng, J. Recent Advances of On-Demand Dissolution of Hydrogel Dressings. *Burns Trauma* **2018**, *6*, 35.
- (36) Konieczynska, M. D.; Villa-Camacho, J. C.; Ghobril, C.; Perez-Viloria, M.; Tevis, K. M.; Blessing, W. A.; Nazarian, A.; Rodriguez, E. K.; Grinstaff, M. W. On-Demand Dissolution of A Dendritic Hydrogel-Based Dressing for Second-Degree Burn Wounds through Thiol-Thioester Exchange Reaction. *Angew. Chem., Int. Ed.* **2016**, *55*, 9984.
- (37) Yuan, L.; Wu, Y.; Fang, J.; Wei, X.; Gu, Q.; El-Hamshary, H.; Al-Deyab, S. S.; Morsi, Y.; Mo, X. Modified Alginate and Gelatin Cross-Linked Hydrogels for Soft Tissue Adhesive. *Artif. Cell Nanomed. Biotechnol.* **2017**, *45*, 76.
- (38) Ghosh, S.; Gayen, P.; Jan, S.; Kishore, A. V.; Kumar, V.; Mallick, A. M.; Mukherjee, A.; Nandi, S. K.; Roy, R. S. Bioinspired Non-Immunogenic Multifunctional Sealant for Efficient Blood Clotting and Suture-Free Wound Closure. *ACS Biomater. Sci. Eng.* **2020**, *6*, 6378.
- (39) Bu, Y.; Shen, H.; Yang, F.; Yang, Y.; Wang, X.; Wu, D. Construction of Tough, in Situ Forming Double-Network Hydrogels with Good Biocompatibility. *ACS Appl. Mater. Interfaces* **2017**, *9*, 2205.
- (40) Li, Z.; Zheng, Z.; Su, S.; Yu, L.; Wang, X. Preparation of A High-Strength Hydrogel with Slidable and Tunable Potential Functionalization Sites. *Macromolecules* **2016**, *49*, 373.
- (41) Zhu, W.; Chuah, Y. J.; Wang, D.-A. Bioadhesives for Internal Medical Applications: A Review. *Acta Biomater.* **2018**, *74*, 1.
- (42) Ghobril, C.; Charoen, K.; Rodriguez, E. K.; Nazarian, A.; Grinstaff, M. W. A Dendritic Thioester Hydrogel Based on Thiol-Thioester Exchange as A Dissolvable Sealant System for Wound Closure. *Angew. Chem., Int. Ed.* **2013**, *52*, 14070.
- (43) Guo, J.; Sun, W.; Kim, J. P.; Lu, X.; Li, Q.; Lin, M.; Mrowczynski, O.; Rizk, E. B.; Cheng, J.; Qian, G.; Yang, J. Development of Tannin-Inspired Antimicrobial Bioadhesives. *Acta Biomater.* **2018**, *72*, 35.
- (44) Srivastava, G. K.; Alonso-Alonso, M. L.; Fernandez-Bueno, I.; Garcia-Gutierrez, M. T.; Rull, F.; Medina, J.; Coco, R. M.; Pastor, J. C. Comparison between Direct Contact and Extract Exposure Methods for PFO Cytotoxicity Evaluation. *Sci. Rep.* **2018**, *8*, 1425.
- (45) Luo, Z.; Jiang, L.; Xu, C.; Kai, D.; Fan, X.; You, M.; Hui, C. M.; Wu, C.; Wu, Y.-L.; Li, Z. Engineered Janus Amphipathic Polymeric Fiber Films with Unidirectional Drainage and Anti-Adhesion Abilities to Accelerate Wound Healing. *Chem. Eng. J.* **2021**, *421*, 127725.
- (46) Hong, Y.; Zhou, F.; Hua, Y.; Zhang, X.; Ni, C.; Pan, D.; Zhang, Y.; Jiang, D.; Yang, L.; Lin, Q.; Zou, Y.; Yu, D.; Arnot, D. E.; Zou, X.; Zhu, L.; Zhang, S.; Ouyang, H. A Strongly Adhesive Hemostatic Hydrogel for The Repair of Arterial and Heart Bleeds. *Nat. Commun.* **2019**, *10*, 2060.